

Synthesis and Performance of Core-Shell Magnetic Alumina Spheres

He Ting-ting¹, Fu Qing-tao^{1*}, Mu shan-liang^{1*}, Liu Chen-guang²

(¹School of Chemistry and Resources Environment, LinYi University, Linyi 276000, China; ²College of chemical engineering, China University of petroleum(east), Qingdao 266580, China)

*corresponding author e-mail: fqtmail@aliyun.com

Abstract. Magnetic alumina micro-spheres with Fe core/Al₂O₃ shell structure were prepared by the oil column method. It shows that the specific surface area and pore volume of the Fe/SiO₂/Al₂O₃ composite micro-spheres calcined at 600°C were 185 m²/g and 0.98 cm³/g, respectively. The specific saturation magnetization is 26.0 emu/g. The distribution of particle size was in the range of 100~200 μm.

1. Introduction

Core-shell composites has recently received much attention, due to the application of these structures in various applications [1-9]. The fabrication of micro-spheres from alumina and magnetic particles has been investigated on account of their unique magnetic responsivity and excellent physical strength [10-12].

It was shown that spindle-shaped magnetite[10] has higher specific saturation magnetization, and coercive force compared with other magnetite. In this work, a new kind of magnetic alumina micro-spheres with spindle-shaped magnetite core can be synthesized by the oil column method.

2. Experimental

2.1 Experimental materials

Sphere-type Fe₂O₃ was purchased from Shanghai Material Corp., China; alumina sol contains 11% aluminum from Beijing technology Co., Ltd. China; hexamethylenetetramine (HMT), tetraethyl orthosilicate (TEOS) and ammonia solution (28 wt%) were from Shanghai ChemicalCorp., China

2.2 Preparation of core-shell Fe₂O₃/SiO₂ composites

Fe₂O₃/SiO₂ composites were prepared according to the reported method. Briefly, 1.25g Fe₂O₃ was dispersed in hydrochloric acid of 1000mL(0.1mol L⁻¹) with ultrasonication and then washed with deionized water. Followedly, the samples was put in homogeneously solution of ethanol (720 mL), water (180mL) and ammonia (10mL of 28wt%) for 0.5h. The reaction was stirred with adding tetraethyl orthosilicate of 2.5g at room temperature and stirred for 6h to obtain sample Fe₂O₃/SiO₂. Then the samples were cleaned by ethanol and deionized water, and dried at room temperature, respectively.



2.3 Preparation of Magnetic Alumina spheres

3g $\text{Fe}_2\text{O}_3/\text{SiO}_2$ was put into 50g aluminum sol by ultrasonic at 10°C . Subsequently, a certain amount of hexamethylene solution with a concentration of 40 wt% (less than 10°C) was added dropwise to the above samples.

Then a homogeneous mixture was obtained by stirring vigorously. The sol mixture was put into vacuum pump oil column (100°C) by a droplet distributor. Lastly, spherical gel was formed by the interfacial tension between sol droplets and oil phase. The samples were aged at 140°C as well as a pressure of 0.5 ~ 0.6 MPa for 6 hours in the autoclave. Lastly, the samples were washed with deionized water. Subsequently, the washed sample was dried at 120°C and calcined at 500°C .

2.4 Analysis and characterization

The X-ray powder diffraction (XRD) were in a Panalytical X'Pert Pro MPD diffract meter. The magnetic properties were using a Lake Shore vibrating sample magnetometer (VSM). Elemental analysis was using a Shimadzu ICPS-75000. A Hitachi S-4800 scanning electron microscope (SEM) and JEM-2100UHR Transmission electron microscope (TEM) was used.

3. Results and discussion

3.1 Characterization of needle Fe_2O_3 and $\text{Fe}_2\text{O}_3/\text{SiO}_2$

The performance of needle Fe_2O_3 particle of coating SiO_2 film was characterized. Then the characterization of the morphology, crystal structure, and magnetic properties of needle Fe_2O_3 and $\text{Fe}_2\text{O}_3/\text{SiO}_2$ were shown in Figure 1 to 4.

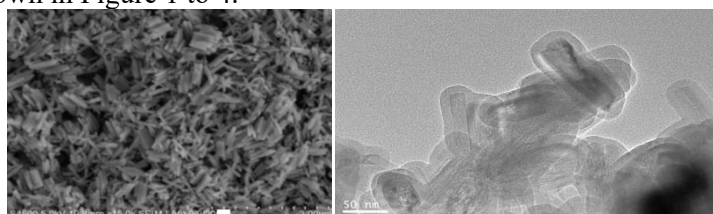


Figure 1 SEM micrographs of $\text{Fe}_2\text{O}_3/\text{SiO}_2$ Figure 2 TEM micrographs of $\text{Fe}_2\text{O}_3/\text{SiO}_2$

The SEM image of $\text{Fe}_2\text{O}_3/\text{SiO}_2$ was shown in Figure 1. The primary particle size of $\text{Fe}_2\text{O}_3/\text{SiO}_2$ is about 100nm. The SEM shows that the sample particle is uniform. TEM image of $\text{Fe}_2\text{O}_3/\text{SiO}_2$ shows that the sample has a core-shell structure in Figure 2. The SiO_2 film is relatively uniform and dense with the thickness of around 15 nm.

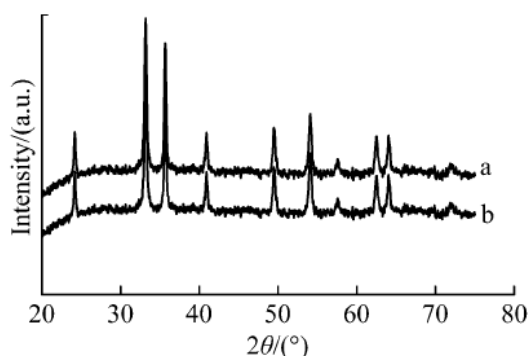


Figure 3 XRD patterns Fe_2O_3 and $\text{Fe}_2\text{O}_3/\text{SiO}_2$

The XRD diffraction patterns of Fe_2O_3 and $\text{Fe}_2\text{O}_3/\text{SiO}_2$ are shown in Figure 3. The characteristic reflections of Fe_2O_3 can be attributed to the diffraction angle (2θ) at 30.3° , 35.7° , 43.3° , 57.3° , and 63.0° , respectively.

The diffraction planes are (220), (311), (400), (511) and (440). The corresponding crystal plane spacing is 0.295nm, 0.252 nm, 0.209 nm, 0.170 nm, 0.161 nm, and 0.148 nm, respectively, belonging to the peak of the Fe_2O_3 crystal phase and $\text{Fe}_2\text{O}_3/\text{SiO}_2$ complex. The characteristic diffraction peaks of

the composite material were similar to that of Fe_2O_3 indicating that no new crystal phase was generated due to the amorphous nature of SiO_2 .

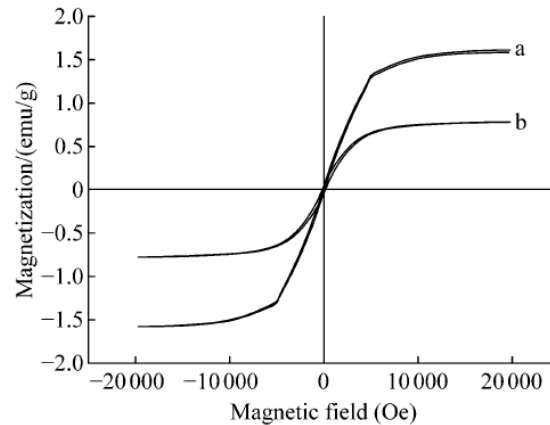


Figure 4 Magnetization hysteresis loops of Fe_2O_3 (a) and $\text{Fe}_2\text{O}_3/\text{SiO}_2$ (b)

The field-dependent magnetization curves of Fe_2O_3 and $\text{Fe}_2\text{O}_3/\text{SiO}_2$ at 300K are presented in Figure 4. Both samples are characteristic of typical ferromagnetic materials with a hysteresis loop. The specific saturation magnetization of $\text{Fe}_2\text{O}_3/\text{SiO}_2$ is lower (0.75 emu/g) corresponding to the Fe_2O_3 (1.75 emu/g). The coercivity force of $\text{Fe}_2\text{O}_3/\text{SiO}_2$ (390 Oe) is slightly smaller than the corresponding Fe_2O_3 (400 Oe). Elemental analysis shows that the weight of Fe_2O_3 in $\text{Fe}_2\text{O}_3/\text{SiO}_2$ sample is 62.8 wt%, which is according to theoretical value of 63 wt%.

3.2. Characterization of $\text{Fe}_2\text{O}_3/\text{SiO}_2/\gamma\text{-Al}_2\text{O}_3$ Magnetic Spheres

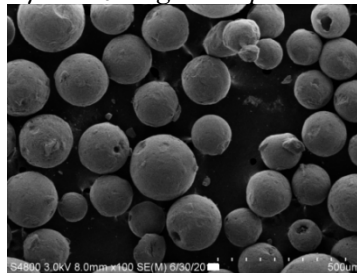


Figure 5 SEM micrographs of magnetic Al_2O_3 micro-spheres

The samples were prepared by oil column method. The results were shown in Figure 5. As can be seen from Figure 5, magnetic alumina spheres were prepared by a rapid dropping method. The magnetic $\text{Fe}_2\text{O}_3/\text{SiO}_2/\gamma\text{-Al}_2\text{O}_3$ micro-spheres have uniform particle size, most of which is in the range of 100~200 μm .

In order to obtain high magnetic alumina micro-spheres, the synthesized micro-spheres were placed in a tubular furnace with a hydrogen gas atmosphere at different reduction temperature. Then the micro-spheres with different magnetization were obtained by reduction at 500 $^\circ\text{C}$ and 600 $^\circ\text{C}$.

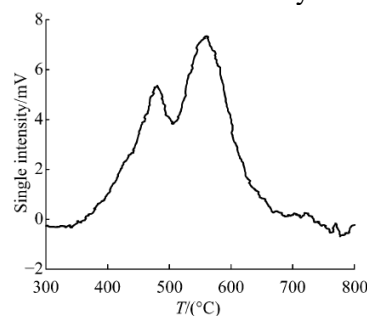


Figure 6 The TPR curve of $\text{Fe}_2\text{O}_3/\text{SiO}_2/\gamma\text{-Al}_2\text{O}_3$ micro-spheres

In the test of the TPR, the synthesized $\text{Fe}_2\text{O}_3/\text{SiO}_2/\text{Al}_2\text{O}_3$ samples were carried out by the mass ratio of $\text{H}_2/\text{Ar}(1: 10)$ in reducing atmosphere. The TPR curve was shown in Figure 6. TPR analysis showed that the two peak with obvious hydrogen consumption at the temperature of 480°C and 560°C . The reduction of former peak should be attributed to Fe_3O_4 . The later peak at 560°C is Fe. The result was according to the results of the literature [10]

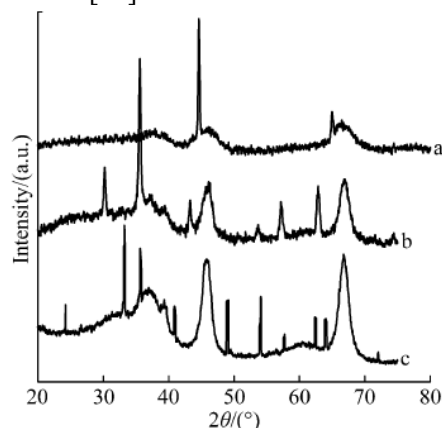


Figure 7 XRD patterns of $\text{Fe}/\text{SiO}_2/\text{Al}_2\text{O}_3$ micro-spheres of a; $\text{Fe}_3\text{O}_4/\text{SiO}_2/\text{Al}_2\text{O}_3$ micro-spheres of b; $\text{Fe}_2\text{O}_3/\text{SiO}_2/\text{Al}_2\text{O}_3$ micro-spheres of c.

In order to further verify the results of TPR, the reduction micro-spheres were analyzed by XRD. Figure 7 (a) shows XRD spectrum of $\text{Fe}/\text{SiO}_2/\text{Al}_2\text{O}_3$ micro-spheres at 600°C . As can be seen from the diagram, $\gamma\text{-Al}_2\text{O}_3$ and Fe diffraction peaks appear at the same time according to the standard card (JCPDS No. 10-0425) and there are no other impurity peaks. This means hydrogen can make $\alpha\text{-Fe}_2\text{O}_3$ complete reduction to a single substance Fe at 600°C . The results was according to the results of TPR analysis. The diffraction angle (2θ) is 46.9° and 66.6° of the two relatively strong $\gamma\text{-Al}_2\text{O}_3$ characteristic peaks, assigned to crystal planes for (400) and (440). The corresponding lattice spacings are 197nm and 0.140nm.

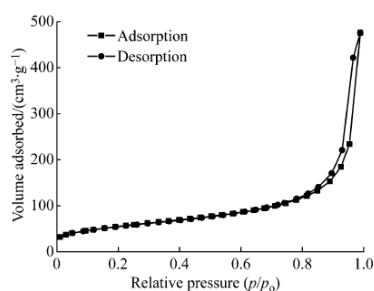


Figure 8 N_2 adsorption-desorption isotherms of $\text{Fe}/\text{SiO}_2/\gamma\text{-Al}_2\text{O}_3$ microspheres

Figures 8 are adsorption-desorption isotherms and pore size distribution curves of magnetic $\text{Fe}/\text{SiO}_2/\gamma\text{-Al}_2\text{O}_3$ spheres. According to the IUPAC standard, magnetic adsorption-desorption isotherms are Type IV, which has a significant hysteresis loop at $P/P_0 = 0.85$ shows due to the capillary condensation phenomenon of the mesopore in the higher pressure. The hysteresis loop is H1 type and H3 superposition.

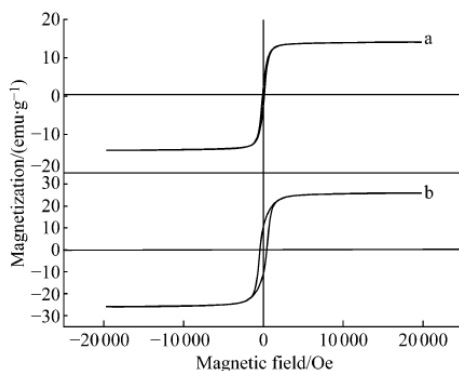


Figure 9 Magnetization hysteresis loops of $\text{Fe}_3\text{O}_4/\text{SiO}_2/\gamma\text{-Al}_2\text{O}_3$ of a; $\text{Fe}/\text{SiO}_2/\gamma\text{-Al}_2\text{O}_3$ of b

Figure 9 shows the magnetic hysteresis of magnetic $\text{Fe}/\text{SiO}_2/\gamma\text{-Al}_2\text{O}_3$ balls. It still has ferromagnetic properties. The saturation magnetization (M_s) and residual magnetism (M_r) of sample is 26 emu/g, 430 Oe, respectively.

4. Conclusions

Alumina micro-spheres with magnetic Fe cores were successfully synthesized. The $\text{Fe}/\text{SiO}_2/\gamma\text{-Al}_2\text{O}_3$ micro-spheres have a high value of specific saturation magnetization of 26 emu/g and low values of coercivity, and they have well-formed spheres with smooth surfaces and a particle size distribution in the range of 100~200 μm . The average specific surface area and total pore volume are 20.6 nm^2/g , 185 m^2/g and 0.98 cm^3/g , respectively. Therefore, the $\text{Fe}/\text{SiO}_2/\gamma\text{-Al}_2\text{O}_3$ micropheres prepared in this work could be utilization in the magnetically stabilized bed technology.

Acknowledgements

This work was supported by Natural Science Foundation of Shandong (No.ZR2015BL023). We are grateful for their financial supports.

References

- [1] Wang C, Wang L, Jin J, et al, *Appli. Cata. B: Environmental*, 2016,188(2): 351-359.
- [2] Zhang W X, Zheng J Z, Shi J G, et al. *Anal. Chimi. Acta*, 2015,853(3):285-290.
- [3] Chen L L, Li X D, Wang Y Q, et al, *J. Power. Sources*. 2014, 272(5):886-894.
- [4] Abdelnasser S S, Ibrahim A A, et al, *Electron. J. Biotech*, 2014,17(6):55-64.
- [5] Salgueirino-Maceira V, Correa-Duarte M A, Spasova M, et al, *Adv. func. Mater*,2006,16(2):509-514.
- [6] Caruso F, Susha A S, Giersig M, et al, *Adv. Mater*,1999,11(4):950-953.
- [7] Cheng B, Zhao L, Yu J G, et al, *Mater. Res. Bull*, 2008,43(2):714-722.
- [8] Zhao W R, Gu J L, Zhang L X, et al, *J. Am. Chem. Soc*, 2005,127: 8916-8917.
- [9] Deng Y H, Qi D W, Deng C H, et al, *J. Am. Chem. Soc*,2008,130:28-29.
- [10] Feng J T, Lin Y J, Li F, et al, *Appl. Catal. A Gen*, 2007,329:112-119.
- [11] Feng J T, Lin Y J, Li F, et al, *Ind. Eng. Chem. Res*, 2009,48:692-697.
- [12] Li Y, Liu Y C, Tang J, et al, *J. Chromatogr. A*, 2007,1172:57-71.